ITER Operation Space in terms of T_e and N_e at the Plasma Edge

G. Janeschitz, A. Hubbard*, Yu. Igitkhanov, J. Lingertat**, T. Osborne***,
H.D. Pacher+, O.P. Pogutse**, D.E. Post, M. Shimada++, M. Sugihara, W. Suttrop+++,

ITER Joint Central Team, Joint Work Site, D-85748 Garching, Germany
** Plasma Science and Fusion Centre, MIT, Cambridge, Ma 02139, U.S.A.*
***JET Joint Undertaking, Abingdon, OX14 3EA, U.K.*
** **General Atomics, CA ..... U.S.A.*

+The NET Team , D-85748 Garching, Germany

++Jaeri, Naka, Ibaraki-ken, Japan

+++Max Planck Institut fuer Plasmaphysik, D-85748 Garching Germany

1 Introduction:

With the advent of improved diagnostic capabilities on several divertor tokamaks, it has recently become possible to define the operational space of H-mode and L-mode in terms of T_e and n_e just inside the separatrix [1], i.e. in terms of the plasma parameters at the top of the H-mode pedestal. From such a diagram we can see that the edge operational space of a particular machine is governed by 4 boundaries (Fig. 1), namely:

- The uppermost boundary divides the unstable from the stable operation space and is defined by the ballooning limit which together with the H-mode pedestal width defines a maximum pedestal temperature for a given density.
- The second boundary determines the transition between Type I and Type III ELMs. Achievement of an H-mode with good confinement requires T close to, or above this boundary, yielding a minimum edge temperature. Thus the intersection of boundary 2 with boundary 1 can be interpreted as an H-mode density limit (Hot density limit [2]).
- The third boundary determines the threshold temperature for the L to H-mode transition.
- The fourth boundary describes the temperature related to the onset of full divertor detachment leading to an X-point marfe (cold edge (L-mode) density limit [2]).

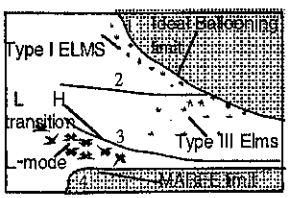

Fig. 1: Schematics of the four boundaries governing the operational space of a machine

In order to predict the operational space for ITER on the basis of edge measurements performed on different machines a theoretical expression for each boundary had to be developed and tested against the data, the width of the H-mode pedestal had to be determined and a scaling of this width to ITER had to be found.

2 Theoretical expressions for the boundaries and for the pedestal width:

Boundary 1 is assumed to be governed by the ideal ballooning limit. We thus evaluate the S-α diagram for each experiment using the analytic formulation in [3].The shear value $S \equiv \overline{\frac{r}{q}\frac{\partial q}{\partial r}}$ required for this calculation is derived from $q_{eff} = \frac{L_0^2 B_T}{2\pi\mu_0 RI}; L_0 = 2\pi a\sqrt{\frac{1+\kappa^2}{2}}$ by introducing a rather broad current density profile. The resulting average shear in the pedestal region varies between ~ 8.5 and ~ 12 depending on the machine and on B_T and I_p for the particular set of discharges. The critical pressure gradient for the onset of type I ELMs and thus for the ballooning limit has been found in several machines to depend on triangularity. In order to take this into account we multiplied "α" from our model with a function derived from a triangularity fit to the results of [4]. Multiplying this marginal pressure gradient by the pedestal width Δ gives the pressure on top of the pedestal, from which the boundary 1 can be plotted assuming a particular ratio between Ti and Te. The above current density profile was derived by adjusting it

until the ASDEX-UP Te values were reproduced with $\Delta = 2.2$ and then kept constant for all machines (for consistency) yielding the discussed shear values (limitation of analytic approach).

The pedestal width can be obtained from measurements or from an analytical expression adjusted to the boundary 1 data. The accuracy of determining Δ from measured data is quite poor in most machines and in order to extrapolate to ITER an analytical expression is needed in any case. Therefore Δ was obtained by fitting an analytic function to the boundary 1 data.

Whereas Te vs ne measured at the pedestal before a type I ELM in ASDEX and to some extent in DIII-D suggest a constant pressure and thus a constant Δ over the whole density range (Fig. 3,4), JET data are better fitted by assuming a temperature dependent Δ [5] (Fig. 5,6). In addition, when plotting the measured Δ_{exp} (tanh fit to data) from DIII-D versus the pedestal temperature a trend for Δ_{exp} to increase with Te-pedestal can be inferred (data scatter is big). We assume also that electron turbulence driven transport (Drift Alfven mode see below and [6]) is stabilised after the L-H transition over a wider range of the minor radius than the pedestal. The width of the H-mode pedestal is therefore probably governed only by the stabilisation of ion turbulence due to poloidal rotation shear (radial electric field) which is observed only over a limited width (e.g. [7]). Assuming further that this width may be related to the banana width and thus to the ion poloidal gyro radius and following the suggestion in [4] we find: $\Delta = f\sqrt{\rho_p R}$ where "f" is a scaling factor (see below) which allows extrapolation to ITER. The factor "f" was adjusted for each machine such that the resulting boundary agrees with the measured data. In addition Δ_{calc} was compared to the experimental values (within a confidence range) in the middle of the density range covered by measurements. The agreement between Δ_{calc} and the experimental values is rather good except for DIII-D where Δ_{exp} is 1 cm to 2 cm (and sometimes 3 cm) and $\Delta_{calc} \sim 4$ cm (Fig. 4) and for C-mod where Δ_{exp} is estimated to be ~8 mm while $\Delta_{calc} = 4$ mm. The differences can probably be explained for both machines with deviations of the critical pressure gradient from the ballooning limit. While DIII-D might enter second stability at the edge [8], C-mod might have gradients below the ballooning limit (no Type I ELMs). Again in order to apply a consistent approach for all machines we nevertheless assumed that the pressure gradients are governed by the ballooning limit. A more accurate evaluation of the width can only be done by sofisticated MHD code calculations (in the future).

A plot of "f" versus minor radius for the different machines is consistent with an approach of "f" to an asymptotic value around 0.275. From this plot it can also be seen that JET is already close to this value and thus ITER should have a value between JET (f=0.26) and the asymptotic limit resulting in "f_{ITER}" ~ 0.27, $\Delta_{ITER} = 9$ cm (Fig. 2). Another way of extrapolating "f" to ITER is using a non linear fit which results in "f"=0.46, $\Delta_{ITER} = 19$ cm (Fig. 2). The reason for choosing the minor radius instead of "R" for the extrapolation is that ASDEX and DIII-D have different "f" and different "a" values but the same "R". With this kind of scaling Δ_{calc} depends on the pedestal temperature and thus varies with density resulting in a boundary 1 which deviates slightly from a constant pressure curve.

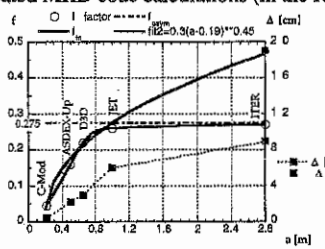

Fig. 2: Two scalings for factor "f" and of the resulting Δ versus minor radius

However, as already indicated above a nonconstant pressure seems not to be a good fit for ASDEX (Fig. 3). A tentative explanation is that due to the relatively low temperature of boundary 1 at high densities the ratio of Ti to Te might vary with density in ASDEX and possibly also somewhat in DIII-D. Thus also the critical gradient for Te will vary and counter balance the variation of Δ. We have therefore introduced a variation of the ratio r=Ti/Te from r=2 at 10^{19} m^{-3} to r=1 at $10^{20}m^{-3}$ in ASDEX and from r=1.5 to r=1 over the same density range for DIII-D. The scatter of the data would allow also for somewhat smaller variations. In the other machines including ITER we assumed that the ratio of Ti/Te is constant over the density range covered which is justified by the high pedestal temperatures found in JET (and predicted for ITER) and the high densities in C-mod. With this assumption the experimental data of all machines is fitted quite well. With the above scaling for "f", boundary 1 for ITER can then be derived.

For Boundary 2 a model is suggested by Igitkhanov and Pogutse relating the threshold temperature to a Tcrit for stabilising a flute dissipative mode which remains unstable above the threshold temperature for the drift Alfven mode (L to H transition [6]). When this expression is adjusted to ASDEX data (at the position of the pedestal), it also fits DIII-D data quite well (Fig. 3,4) but not JET (ITER) and C-mod for which a different multiplication factor which does not scale with the pedestal width would be needed. Further investigations are needed to predict the intersection point between boundary 1 and 2 and thus the H-mode density limit for ITER.

Boundary 3 is defined by the critical temperature at the position of the pedestal above which the drift Alfven mode is stabilised $T_{cr} = \left[sB\frac{I}{a^2}\right]^{f1} \frac{A^{-f2}}{n^{f3}} f_4 \Delta_{calc}$ where "f1", "f2", "f3", "f4" are weak functions of density as defined in [6]. As can be seen from Fig. 3 to 7 theory, and data agree quite well in all machines.

A qualitative physics picture of the H-mode could be that stabilisation of both electron and ion turbulence is required to establish the transport barrier. Ion turbulence is stabilised by poloidal rotation shear but during L mode Δ and the electric field are small [7] and the electron turbulence due to the drift Alfven mode may dominate transport in the edge region. When the heating power is increased the temperature at the edge increases, Δ and the electric field increase somewhat, but no large effect is expected (observed) on transport. Only when the drift Alfven mode is stabilised and thus electron transport is strongly reduced a sudden further increase of the edge (pedestal region) temperature and density becomes possible. As a result Δ and the region of electric field shear grows, increasing the width over which ion turbulence is stabilised by poloidal rotation shear. Therefore the drift Alfven mode becomes the important trigger mechanism [6] but the H-mode transport barrier develops only in the region where both electron and ion turbulence are stabilised and thus over the width defined by the poloidal rotation shear. However, confinement also improves in the core if the critical temperature gradient for ion turbulence is determined by the boundary condition (temperature) on top of the H-mode pedestal as suggested in [9].

The fourth boundary is derived from a set of analytic equations (two point model [10]) describing the onset of full divertor detachment leading to an X-point marfe (cold edge (L-mode) density limit). Calculations performed for ASDEX fit the measured data quite well and suggest that the boundary derived for ITER should be a good approximation. As can be seen from Fig. 8 the cold density limit should not pose any problems for ITER.

3 Discussion and Conclusions:

As one can see from Fig. 3 to 7 the theoretical expressions and the data agree quite well and thus give confidence for the extrapolation to ITER. The absolute values of temperature versus density for ballooning and L-H mode transition in ITER depend on the extrapolated pedestal width (Fig. 8) for which presently no theory exists and which therefore remains uncertain. However, due to the fact that these values are derived from a critical gradient times Δ, an uncertainty in the prediction of Δ only shifts the operation space temperature up and down but does not change its shape. Also results from transport codes which might use the derived expressions for calculating e.g. the H-mode power threshold (future plans) will therefore not depend strongly on the predicted width. Another important feature which can be seen from the comparison of two different triangularities (δ=0.21, δ=0.31) in JET (Fig. 5) is that discharges with higher triangularity allow H-mode operation at temperatures above Tcrit for Type III ELMs at higher density (higher H-mode density limit) pointing towards the importance of achieving reasonable high triangularity also in ITER (δ~0.25). The relatively high value of Tcrit for Type III ELMs as seen in JET (~ 3keV, BT=3.5T, Fig. 5) would result for ITER in an estimated H-mode density limit of ~ $6 \times 10^{19} m^{-3}$ at the top of the pedestal when the ratio of the two Δs is used for extrapolation. The triangularity of δ ~0.25 in ITER, higher than that of JET (δ ~0.21), might increase this value to ~ $7 \times 10^{19} m^{-3}$ implying a line average density of ~ $0.91 \times 10^{20} m^{-3}$, i.e. 11% above the Greenwald density. However due to the lack of a model for Type III ELMs the exact extrapolation and thus the H-mode density limit for ITER remains unknown.

It is a clear conclusion that the temperature on top of the H-mode pedestal is ~ 4 to 8 keV at the H-mode density limit and higher at lower densities. These values are higher by more than an order of magnitude than the value assumed in [11] ($T_{pedestal}$ = 300 eV) which was used in the model of [9] to predict a confinement for ITER well below the one obtained from the global scaling laws. If the pedestal temperatures obtained from our scaling were taken as boundary

conditions it is likely that even this model would predict adequate confinement values for ignited operation in ITER.

4 References:

[1] M. Kaufmann et al, Proc. 16th IAEA Fusion Energy Conf., paper O1-5 Montréal 1996
[2] G. Janeschitz, et. al., Proc. 16th IAEA Fusion Energy Conf., paper A1-6 Montréal 1996
[3] O. Pogutse and E. Yurchenko, *Reviews of Plasma Physics*, Vol. 11, pp. 65-148.
[4] Y. Kamada et al, Proc. 16th IAEA Fusion Energy Conf., paper A1-6 Montréal 1996
[5] J. Lingertat, et.al., this conference
[6] O.P. Pogutse, et.al. this conference
[7] R. J. Groebner, et. al., Proceedings 16th EPS Conf., Petit-Lancy, Switzerland, 1989
[8] T. Osborne, et.al., this conference
[9] M. Kotschenreuther, W. Dorland, et. al., Physics of Plasmas 2 (6) June 1995
[10] M. Sugihara et al, Proc. 12th Int. Conf. Plasma-Surface Interactions, St. Raphael 1996
[11] Glanz, Science Magazine December 1996

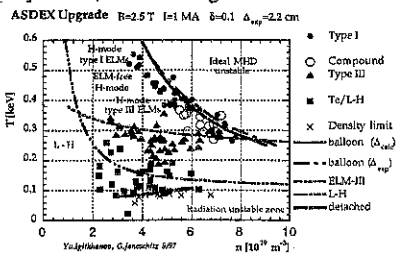

Fig.3: Operation space for ASDEX-Upgrade. The good agreement between data and theory can be seen. Type III ELM curve adjusted.

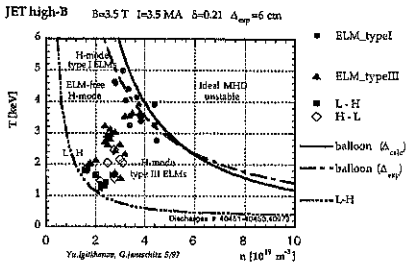

Fig. 6: The JET high field operation space shows a relatively high threshold Temperature for Type III ELMs.

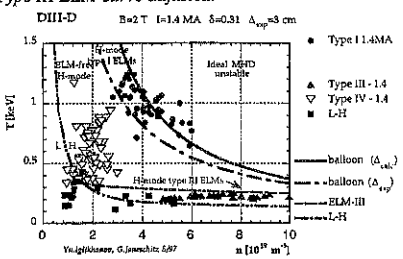

Fig. 4: Operation space for DIII-D, good agreement of data and theory except for the "Δ = 3 cm" ballooning curve (dashed).

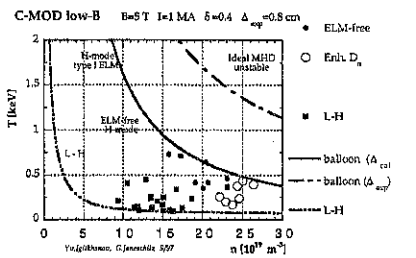

Fig. 7: C-mod operation space for BT=5T. Good agreement of theory (L-H and Δcalc ~ 4mm) and data except for the dashed curve representing Δexp = 8mm

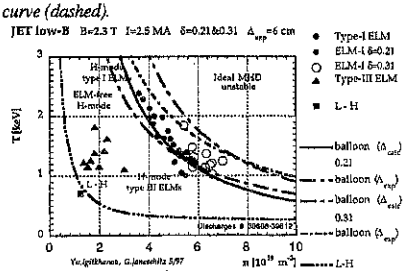

Fig. 5: JET low field operation space. The increase of the operation space (i.e. the H-mode density limit) with triangularity can be seen

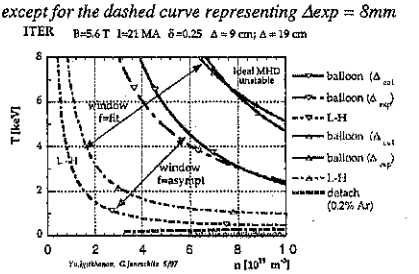

Fig. 8: ITER operation space for "f"=0.46, giving the higher temperatures, Operation space for "f"=0.27 gives T a factor two lower for ballooning and L-H